

Beam-Driven Acceleration in Ultra-Dense Plasma Media

Young-Min Shin^{a),b)},

^{a)}Department of Physics, Northern Illinois University, Dekalb, IL, 60115, USA

^{b)}Accelerator Physics Center (APC), Fermi National Accelerator Laboratory (FNAL),

Batavia, IL, 60510, USA

Accelerating parameters of beam-driven wakefield acceleration in an extremely dense plasma column has been analyzed with the dynamic framed particle-in-cell plasma simulator, and compared with analytic calculations. In the model, a witness beam undergoes a TeV/m scale alternating potential gradient excited by a micro-bunched drive beam in a 10^{25} m^{-3} and $1.6 \times 10^{28} \text{ m}^{-3}$ plasma column. The acceleration gradient, energy gain, and transformer ratio have been extensively studied in quasi-linear, linear-, and blowout-regimes. The simulation analysis indicated that in the beam-driven acceleration system a hollow plasma channel offers $\sim 20\%$ higher acceleration gradient by enlarging the channel radius (r) from $0.2 \lambda_p$ to $0.6 \lambda_p$ in a blowout regime. This paper suggests a feasibility of TeV/m scale acceleration with a hollow crystalline structure (e.g. nanotubes) of high electron plasma density.

Shock waves in an ionized plasma media, excited by relativistic particles, have been of great interest on account of their promise to offer extremely high acceleration gradients of G_0 (max. gradient) = $m_e c \omega_p / e \approx 96 \times n_0^{1/2}$ [V/m], where $\omega_p = (4\pi n_p e^2 / m_e)^{1/2}$ is the electron plasma frequency and n_p is the ambient plasma density of [cm^{-3}], m_e and e are the electron mass and charge, respectively, and c is the speed of light in vacuum. Normally, plasmas in ionized gas have an electron density of $n_p = 10^{17} - 10^{18} \text{ cm}^{-3}$, which in principle thus enables to create wakefields of 30 – 100 GeV/m [1 – 3]. The nonlinear ponderomotive force of a high power laser [4] or the repulsive space charge force of a particle beam [5] can generate plasma wakes resonating with high energy particles. The laser-driven acceleration was first proved by the experiment demonstrating 1 GeV electron energy over a cm long plasma tube, excited by a 40 TW pulse laser in 2006 [6]. The beam-driven acceleration was demonstrated in 2007 by energy doubling experiment with a 42 GeV electron beam in a meter long plasma: a small portion of the bunch tail gains acceleration energy from the oscillating plasma wave excited by the bunch head [7]. These results attracted a significant amount of interest in the development of high-gradient plasma wakefield accelerators [8 – 10]. With the laser pumping method [11, 12], a plasma can hold transverse and longitudinal wakefields of extremely large gradients at the laser-plasma coupling condition. However, to hold the ultimate gradients, for electrons the acceleration requires a high power laser source to compensate for radiation losses. The laser driving method thus fits for heavy particles such as muons or protons that have relatively small radiation losses. For positrons or electrons, the beam-driven acceleration is more appropriate as the energy losses of a drive beam can be transformed into acceleration energy of a witness beam [13]. In general,

acceleration parameters are mainly determined by the degree of beam-plasma synchronization, i.e. phase velocity, v_p , of the plasma wave relative to beam velocity v_b of the plasma wave. Electrons in the relativistic regime move faster than the plasma wave and they undergo phase slippage from the accelerating to the decelerating phase region of the plasma wave. The phase slippage limits the energy gain to $\gamma_p^2 m_e c^2 (G_p/G_0)$ over a dephasing length (l_d) $\sim \gamma_p^2 \lambda_p$, where G_p is the electric field amplitude of the plasma wave and $\gamma_p = (1 - v_p^2/c^2)^{-1/2}$. A high power laser with a short pulse ($< \lambda_p$) can drive a plasma accelerator with relatively slow plasma wave ($\gamma_p \sim 10 - 100$) and the energy gain could be limited by dephasing [13]. For a plasma acceleration driven by a highly relativistic electron beam ($\gamma_b > 100$) with a bunch length shorter than the plasma wavelength ($< \lambda_p$), a plasma wave, however, moves with the beam, so its speed could be sufficiently high ($v_p \sim c$) as to avoid dephasing problem. Such short bunches with a bunch length ranging from sub-100 μm to sub-100 nm can be produced by modulating charge density with a slit-mask [14, 15] or laser-induced micro-bunching techniques [16, 17].

This paper presents the dynamics of wakefield accelerations in dense plasma media, analyzed by the beam-driven plasma wakefield acceleration simulator. The results include spatiotemporal charge and energy distributions of accelerated bunches under various plasma-beam coupling conditions. The paper will culminate with the discussion of some feasible ways of creating a high density plasma channel for high gradient wakefield acceleration.

Since parametric dynamics of relativistic bunches in a dense plasma wave is of interest, several different plasma systems are considered for beam-driven acceleration simulations, including both single and multiple drivers, with bunch parameters. Figure 1 shows the model of the plasma column with multi-bunch excitation under acceleration: (a) 3D contour plot of electric fields from the plasma column and electron bunches and (b) its projected disturbances on the two-dimensional charge density distribution in the plasma and beam frames. In a given system, the electron bunches in the head of the bunch train creates plasma wakes, lose their kinetic energies and the ones in the tail synchronized with phase velocity of the plasma wave gain their energies when coupled with the wake. As shown in Fig. 1(b), multiple drive bunches, spaced with d_{mb} , are injected into a dense plasma, which are followed by a witness bunch injected within the distance of $1 - 1.6 \lambda_p$, where λ_p is the plasma wavelength. In order to examine multi-bunch driven wakefield acceleration over a wide range of electron beam energy, three different beam energies, 50 MeV (low-relativistic), 300 MeV (relativistic), and 850 MeV (ultra-relativistic), are considered for experimental tests with a high energy beam test facility [18, 19]. As extremely dense plasmas in a level of solid-state electronic density are of interest in examining ultra-high gradient accelerations [20, 21], two plasma densities, 10^{25} m^{-3} and $1.6 \times 10^{28} \text{ m}^{-3}$, probably low and high margins of electron density in most of the crystals, are examined with a high energy electron beam in the simulations. Figure 1(b) is a typical simulation result with the plasma resonance condition: 10 bunches of $n_b/n_p \sim 1$ ($d_{mb} \sim \lambda_p$) and $\sigma_r \sim 0.1 \lambda_p$, where σ_r is the bunch radius and n_b is the beam charge density defined in a Gaussian bunch of σ_r . Note that bunches in the train are exactly positioned at the anti-nodes of the plasma beat-waves,

continuously transforming energy from the head to the tail. The solitonic waves of the density fluctuation also induce the strong focusing field squeezing bunches into the cavities. It influences a bunch shape, causing variation of the bunch-to-bunch beam envelope. The field strength gets gradually larger down the wake stream. It should be also noted that some electrons stripped off from the drive bunch by the head-on collision into the uniform plasma are pulled back to the next bunch by attractive forces along the potential lines of the cavity surface. Back-streaming increases charge density of the subsequent bunches, increasing the beam energy losses of drive bunches. The witness beam rapidly loses transverse momentum converted to growing the longitudinal energy spread as it is accelerated by energy gain transformed from the drive bunches. The transverse focusing dominantly appears with the resonant excitation, while it is weaker with excessively dense plasma in the blowout regime. In a real plasma accelerator with the high charge density, the collisional effect could be a critical problem: A scattering rate increased by a large amount of particle-collision diffuses pitch-angle within distances of acceleration energy gain, eventually expelling particles from driving fields. This collisional impact could be avoided or substantially reduced by accelerating particles along a channeling structure such as natural or synthetic crystals (e.g. silicon, germanium, carbon nanotubes, etc) [22 – 24].

The periodic perturbation effect of multi-bunch excitation on wakefield acceleration is analyzed with respect to bunch charge density. Figures 2 and 3 show acceleration gradient and energy gain versus beam charge density, normalized by two plasma number densities, 10^{25} m^{-3} and $1.6 \times 10^{28} \text{ m}^{-3}$, which might be in the lower and upper limits of electron density of solid-state media. The corresponding plasma wavelengths are $10 \text{ }\mu\text{m}$ and 0.264

μm , which are selected as they are also in the spectral range of available photon driving sources such as IR/UV lasers or magnetic undulators [25]. The bunch charge density, n_b , is swept from $0.01 n_p$ to $1000 n_p$, ranging from the under-coupled regime to blowout one. With the simulation conditions, 10 micro-bunches are specified to move through a $10\lambda_p$ thick plasma channel. In the graphs, (1) (and (4)), (2) (and (5)), and (3) (and (6)) are at in-between quasi-linear and linear regimes, middle of the linear regime, and in-between linear and blowout regimes with the two density conditions, respectively. Solid circles, empty circles, and crosses represent 50 MeV, 300 MeV, and 850 MeV respectively, and the solid red line is a theoretical energy gain curve. In the figure, the linear gains are the acceleration field amplitudes (Fig. 2) multiplied by the plasma accelerator length and the nonlinear gains are the measured beam energies in the simulations. Note that the acceleration gradient and energy-gain graphs of wakefield simulations agree well with that of theory in the linear regime. In the under-coupled (off-resonance) regime, (1) and (4), the Gaussian bunch shape is deformed to an asymmetric one due to scatterings that are unsynchronized with a plasma oscillation. The acceleration gradients and energy gains of the simulations are closer to the theoretical ones as the bunch charge density is increased from the quasi-linear regime to linear and blowout regimes ($n_b/n_p > 10$). The maximum acceleration gradients of linear regimes, (2) and (5), range $\sim 0.2 \text{ TeV/m}$ with $n_p = 10^{25} \text{ m}^{-3}$ and $\sim 10 \text{ TeV/m}$ with $n_p = 1.6 \times 10^{28} \text{ m}^{-3}$, which correspond to energy gains of 24.5 MeV and 27 MeV with a length of $10\lambda_p$, respectively. The acceleration gradients of a dense plasma state are 4 – 5 orders of magnitude higher than those of plasmas in gas-state. Figures 4(2) and (5) show that the electron bunches in the tails strongly resonate with traveling disturbances in the plasmas,

generated by a drive bunch, in agreement with the theoretical prediction. It is a completely different pattern from the under-coupled accelerations, (1) and (4), as beam energy is transformed from bunch to bunch via ambient plasmas. This resonance interaction becomes quickly broken with the bunch charge density, n_b , exceeding $\sim 10n_p$, saturating acceleration gradients and energy gains, as shown in Figures 4(3) and (6). In the blowout regime, the excessive space charge force expands the cavity volume beyond the beam modulation wavelength. It results in off-resonance coupling, accompanied by phase slippage, which is mainly ascribed to the saturation of energy gain. The saturation appears at relatively lower bunch charge density with the multiple-bunch driver than a single one due to the greater amount of total charge.

Extending the numerical analysis on the multi-bunch acceleration, the micro-bunched drive acceleration is examined by optimizing the bunch-to-bunch distance. The distance between the two beams ($\sigma \sim 0.1\lambda_p$), driver and witness, was swept from $1.3 - 1.7\lambda_p$, where λ_p is the plasma wavelength, with the bunch charge density of plasma resonance condition. As shown in Fig. 5, acceleration gradient increased steeply from 12 TeV/m with $1.3\lambda_p$ to 18.5 TeV/m with $1.6\lambda_p$, likewise the transformer ratio ($R = E_+/E_-$), which is the ratio between the peak accelerating field (E_+) and decelerating field (E_-) in the distributed beam driving itself in a self-acceleration process of modulated beam [7, 26]. As It appears that both the gradient and transformer ratios drop off if the distance exceeds $1.6\lambda_p$. With a channel length of $10\lambda_p$ and $n_p = 10^{25} \text{ m}^{-3}$, the maximum gradient and transformer ratio with the distance $\sim 1.6\lambda_p$ is 18.5 TeV/m and 57.5 %, respectively. Normally, the acceleration gradient of plasma waves becomes maximized at $\sim 1.5 \lambda_p$ where

the maximum repulsive separation of charged ions occurs. The witness beam is thus optimally synchronized with the plasma wave in the acceleration region. The limited performance of the wakefield acceleration in the dense plasma is mainly attributed to exceptionally intense plasma-electron scatterings, which might cause excessively large phase slippage and energy dispersion. A hollow plasma channel has thus been investigated as expectedly undergoing less collisional scatterings with a high charge density beam than a homogeneously filled column does.

Figure 6 shows time-tagged snapshots of a two-beam accelerating system with a $\sim 10\lambda_p$ hollow plasma channel that is modeled with $n_p \sim 10^{25} \text{ m}^{-3}$. The simulation condition also includes the drive-witness coupling distance of $\sim 1.6\lambda_p$, $\sigma = \sim 0.1\lambda_p$, and a linear regime bunch charge density of $n_b \sim n_p$. For this simulation, the plasma channel is designed with a tunnel of $r = 0.1\lambda_p$. Just like a uniformly filled one, the drive bunch generates tailing wakes in the hollow channel due to the repulsive space charge force. The plasma waves travel along the hollow channel with the density modulation in the same velocity with the witness beam. Note that the bunch shape of the drive beam in the tunnel remains relatively longer than in the cylindrical plasma column. The energy versus distance plots in Fig. 6 (bottom) shows that sinusoidal energy modulation apparently occurs in the plasma channel perturbed by two bunches. Here, the relative position of the drive beam corresponds to the first maximum energy loss, while that of the witness beam does to the first maximum energy gain. The traveling wakes around the tunnel continuously transform acceleration energy from the drive beam to the witness one. The energy gain and acceleration gradient are fairly

limited by the radius and length of the tunnel with respect to plasma wavelength and bunch charge density.

Bunch parameters of the beam-driven acceleration system have thus been analyzed with various tunnel radii, as shown in Fig. 7. For the analysis, the bunch charge density was swept from 1 to 300, normalized by plasma density, n_p , for five different tunnel radii from 0.2 to $0.6\lambda_p$ and relativistic beam energy 20 MeV. While in the linear regime $n_b = \sim 1 - 10n_p$, the maximum acceleration gradient drops off with an increase of the tunnel radius from 0.2 to 0.6, it increases in the blowout regime, $n_b = \sim 10 - 100n_p$. The maximum acceleration gradient is increased from ~ 0.82 TeV/m of $r = 0.2 \lambda_p$ to ~ 1.02 TeV/m of $r = 0.6 \lambda_p$ with $n_b = 100n_p$, corresponding to ~ 20 % improvement. The energy transformer ratio follows a similar tendency with the acceleration gradient curve in the linear and blowout regimes. In the linear regime ($n_b/n_p \sim 1 - 10$), scattering is negligibly small, which does not perturb particle distribution of the bunch within the hollow channel. The repulsive space charge force between the bunch and the plasma is increased in the inversely proportional to their spacing. The channeled bunch thus undergoes the higher acceleration gradient as the channel gets smaller, as shown in Fig. 7. However, in the blowout regime ($n_b/n_p \sim 10 - 100$) the repulsive space charge force from an excessive amount of the bunch charge density against the plasma channel is strong as to heavily perturb the bunch and to scatter electrons out of the bunch. The strength of space charge force is decreased with the channel radius, so the electrons in the bunch is less scattered with an increase of the channel radius. The gradient is thus lowered with an increase of the channel radius accordingly. The similar tendency also appears on the transformer ratio, as shown in Fig.

7(b). The energy is more efficiently converted from the drive beam to the witness one with the larger channel in the blowout regime, although the transformer ratio does not similarly follow the tendency of accelerating gradient with the channel size in the linear regime. The un-similarity between the acceleration gradient and transformer ratio with respect to the channel size in the linear regime might be attributed to the insufficient channel length, $10\lambda_p$. The plasma oscillation from the small bunch charge density is not strong enough to properly convert the beam energies from deceleration to acceleration. The result implies that a hollow channel thus has a higher gradient than a homogeneously filled plasma column in the blowout regime, and the plasma wakefield acceleration gradient is effectively increased by enlarging the channel size. This result opens the possibility of controlling beam parameters of plasma accelerators for higher gradient and large energy conversion efficiency.

In summary, a wide range of beam-driven wakefield acceleration has been parametrically analyzed in dense plasma structures excessively higher than a typical plasma density level, $10^{16} - 10^{18} \text{ m}^{-3}$, of ionized gas, which usually limits obtainable acceleration gradient below 100 GeV/m. In dynamic plasma theory, an ultra-high electric field in tera-electron volt per meter (TeV/m) scale can be produced by a $10^{25} - 10^{28} \text{ m}^{-3}$ range of plasma density. The numerical analysis with a plasma wakefield simulator, designed with dynamic PIC-computational platform, showed a TeV/m range of a single-bunch driver and a multi-bunched driver beam with plasma under optimized coupling conditions in the quasi-linear, linear, and blowout regimes, which agreed well with the linear plasma theory. It turned out that in the dense plasma interaction, a hollow channel is more efficient in controlling beam

parameters and increasing the acceleration gradient and transformer ratio in the blowout regime. In reality, the extremely dense plasma state can be created in solid state materials, in particular when high energy particles are channeled through a crystal. Also, crystalline nanostructures, e.g. carbon nanotubes, have a hollow plasma charge distribution of high density and their density profiles can be readily designed and fabricated. The results thus indicated that the beam-driven channeling acceleration in crystalline media is a viable concept to realistically achieve a TeV/m level acceleration gradient.

ACKNOWLEDGMENT

This work was supported by the DOE contract No. DEAC02-07CH11359 to the Fermi Research Alliance LLC.

References

- [1] T. Tajima and J. M. Dawson, *Phys. Rev. Lett.* 43 (4), 267 (1979)
- [2] J. B. Rosenzweig, D. B. Cline, B. Cole, H. Figueroa, W. Gai, R. Konecny, J. Norem, P. Schoessow, and J. Simpson, *Phys. Rev. Lett.* 61, 98 (1988)
- [3] C. Joshi and T. Katsouleas, *Physics Today* 56 (6), 47 (2003)
- [4] C. Joshi, W. B. Mori, T. Katsouleas, J. M. Dawson, J. M. Kindel, D. W. Forslund, *Nature* 311, 525 (1984)
- [5] C. Joshi, *Phys. Plasmas* 14, 055501 (2007)
- [6] W. P. Leemans, B. Nagler, A. J. Gonsalves, Cs. Toth, K. Nakamura, C. G. R. Geddes, E. Esarey C. B. Schroeder, and S. M. Hooker, *Nature Physics* 418, 696 (2006)
- [7] I. Blumenfeld, C. E. Clayton, F.-J. Decker, M. J. Hogan, C. Huang, R. Ischebeck, R. Iverson, C. Joshi, t. Katsouleas, N. Kirby, W. Lu, K. A. March, W. B. Mori, P. Muggli, E. Oz, R. H. Siemann, D. Walz, and M. Zhou, *Nature* 445, 741 (2007)
- [8] C. Joshi, "Plasma Accelerator", *Scientific American*, 294, 40 (2006)
- [9] C. Joshi and V. Marika, *New J. Phys.* 12, 045003 (2010)
- [10] C. B. Schroeder, E. Esarey, C. G. R. Geddes, C. Benedetti, and W. P. Leemans, *Phys Rev. ST Accel. Beams* 13, 101301 (2010)
- [11] J. Badziak, S. Borodziuk, T. Pisarczyk, T. Chodukowski, E. Krousky, K. Masek, J. Skala, J. Ullschmied, and Yong-Joo Rhee, *Appl. Phys. Lett.* 96, 251502 (2010)
- [12] F. Fang, C. E. Clayton, K. A. Marsh, A. E. Pak, J. E. Ralph, N. C. Lopes, and C. Joshi, *Plasma Phys. Control. Fusion* 51, 024003 (2009)
- [13] G. Xia, D. Angal-Kalinin, J. Clarke, J. Smith, E. Cormier-Michel, J. Jones, P. H.

- Williams, J. W. McKenzie, B. L. Militsyn, K. Hanahoe, O. Mete, A. Aimidula, C. P. Welsch, *Nuclear Instruments and Methods in Physics Research A* 740, 165 (2014)
- [14] D.C.Nguyen, B.E.Carlsten, *NIM-A* 375, 597-601 (1996)
- [15] P. Muggli, V. Yakimenko, M. Babzien, E. Kallos, and K. P. Kusche, *Phys. Rev. Lett.* 101, 054801 (2008)
- [16] R. Palmer, *Journal of Applied Physics* 43, no.7, 3014 (1972).
- [17] L. C. Steinhauer, and W. D. Kimura, *Phys. Rev. ST Accel. Beams* 2, no.8 (1999).
- [18] C. B. Schroeder, C. Benedetti, E. Esarey, F. J. Gruner, W. P. Leemans, *Phys. Rev. Lett.* 107, 145002 (2011)
- [19] C. R. Prokop, P. Piot, B. E. Carlsten, and M. Church, *Nuclear Instruments and Methods in Physics Research A* 719, 17 (2013)
- [20] D. Mihalcea, P. Piot, and P. Stoltz, *Phys. Rev. ST AB* 15, 081304 (2012)
- [21] P. Chen and R. Noble, "Channel Particle Acceleration By Plasma Waves in Metals", slac-pub-4187
- [22] V. D. Shiltsev, *Physics - Uspekhi* 55 (10) 965 (2012)
- [23] T. Tajima and M. Cavenago, *Phys. Rev. Lett.* **59**, 1440 1987
- [24] P. Chen and R. J. Noble, *AIP Conf. Proc.* **396** and **398**, 95 1997
- [25] I. Y. Dodin, N. J. Fisch, *Phys. Plasmas* 15, 103105 (2008)
- [26] P. Chen, D. B. Cline, and W. E. Gabella, *SLAC-PUB-6020* (1992)

Figure Captions

FIG. 1 Simulation of the beam-driven oscillation at resonant condition ($n_b = n_p$) (a) 3D contour plot of longitudinal electric field of plasma channel (b) the density distribution of the electron pulse and the plasma electrons at the head of the micro-bunch train

FIG. 2 Acceleration gradient versus normalized charge distribution graphs of multi-bunched drive beam with 50 MeV, 300 MeV, and 850 MeV (a) $n_p = 10^{25} \text{ m}^{-3}$ and (b) $n_p = 1.6 \times 10^{28} \text{ m}^{-3}$.

FIG. 3 Linear and nonlinear energy gain versus normalized bunch charge density graphs of multi-bunched drive beam with 50 MeV, 300 MeV, and 850 MeV (a) $n_p = 10^{25} \text{ m}^{-3}$ and (b) $n_p = 1.6 \times 10^{28} \text{ m}^{-3}$. The red line is the theoretical curve.

FIG. 4 Two dimensional charge distributions of under-coupled, linear, and blowout regimes of $n_p = 10^{25} \text{ m}^{-3}$, (1) – (3), and $n_p = 1.6 \times 10^{28} \text{ m}^{-3}$, (4) – (6), respectively.

FIG. 5 Acceleration gradient and transformer ratio of two beam plasma acceleration versus bunch-to-bunch distribution normalized by plasma wavelength ($n_p = n_b = 10^{25} \text{ m}^{-3}$)

FIG. 6 Time-tagged charge distribution of a hollow plasma acceleration ($n_p = n_b$) with a drive and witness beam (top) 3D charge distribution (middle) 2D distribution (bottom) spatial energy distribution

FIG. 7 (a) maximum acceleration gradient and (b) transformer ratio versus bunch charge distribution normalized by bunch charge density with various tunnel radii ($r = 0.2 - 0.6\lambda_p$)

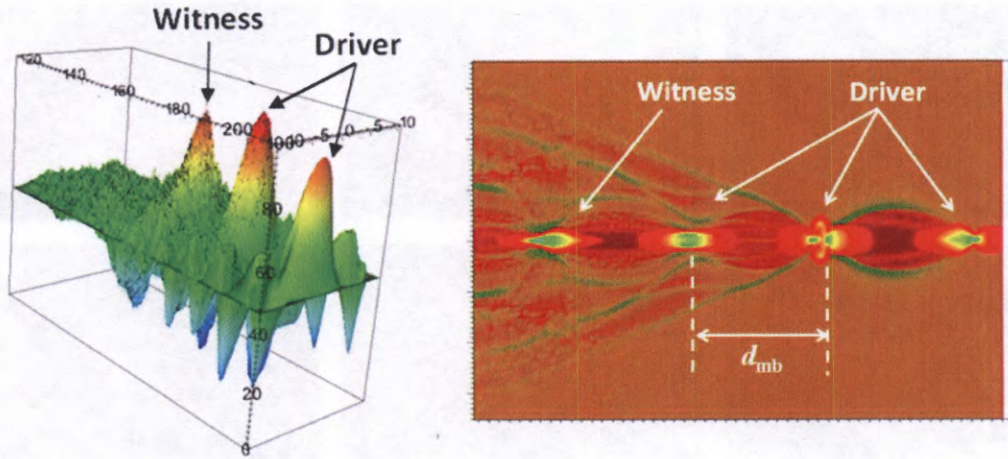


FIG. 1 (Y. M. Shin)

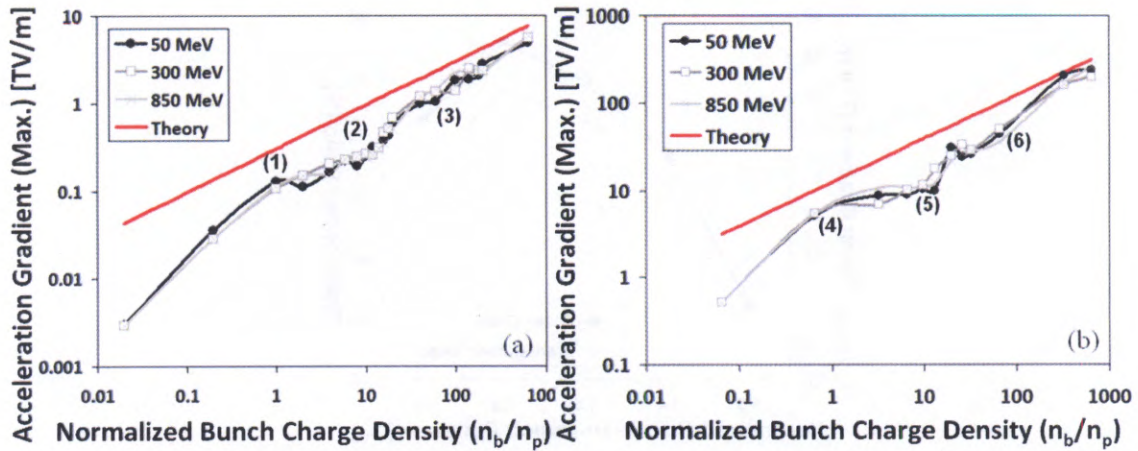


FIG. 2 (Y. M. Shin)

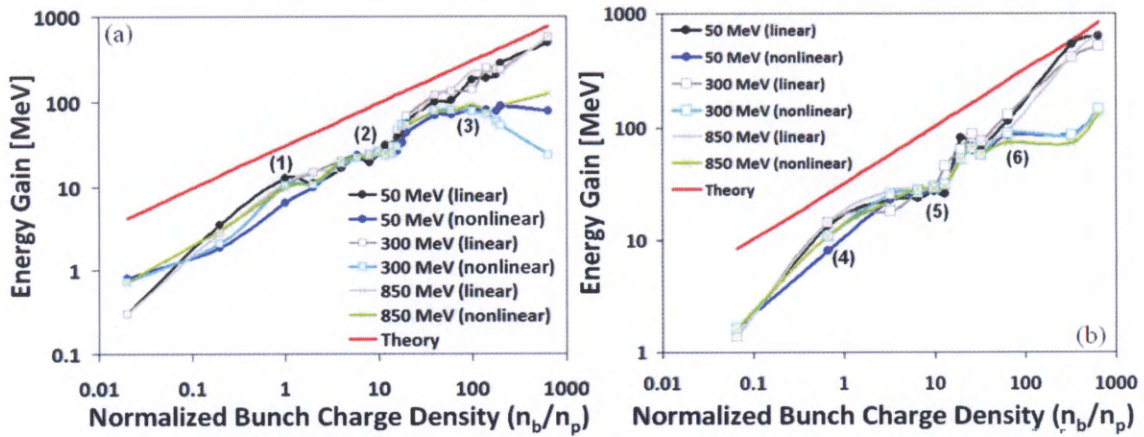


FIG. 3 (Y. M. Shin)

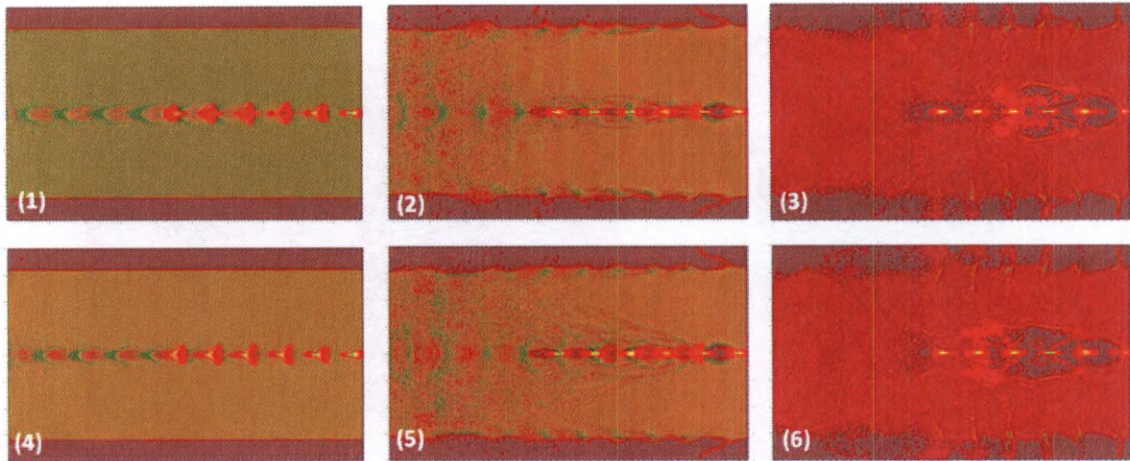


FIG. 4 (Y. M. Shin)

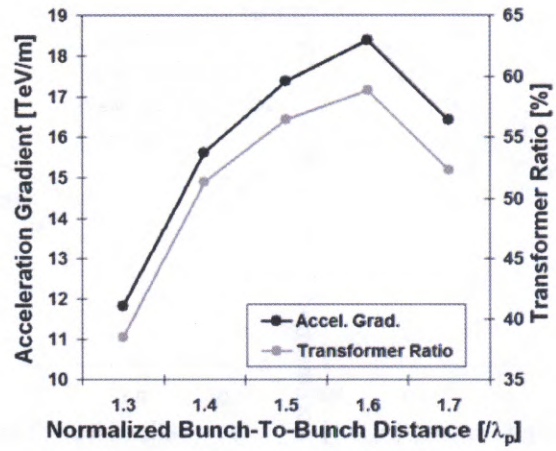


FIG. 5 (Y. M. Shin)

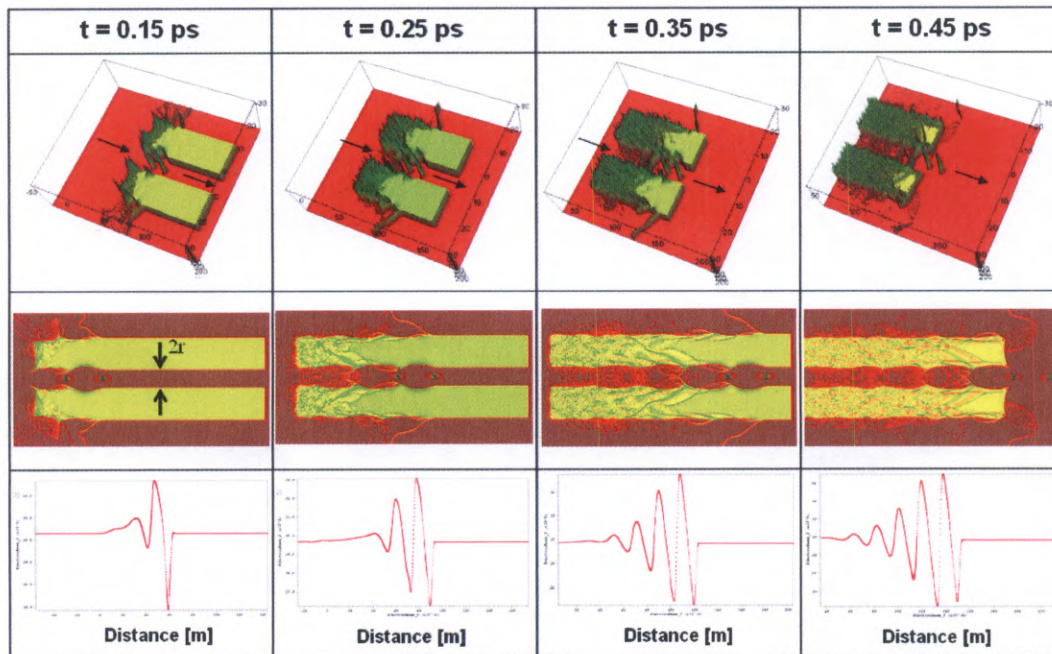


FIG. 6 (Y. M. SHIN)

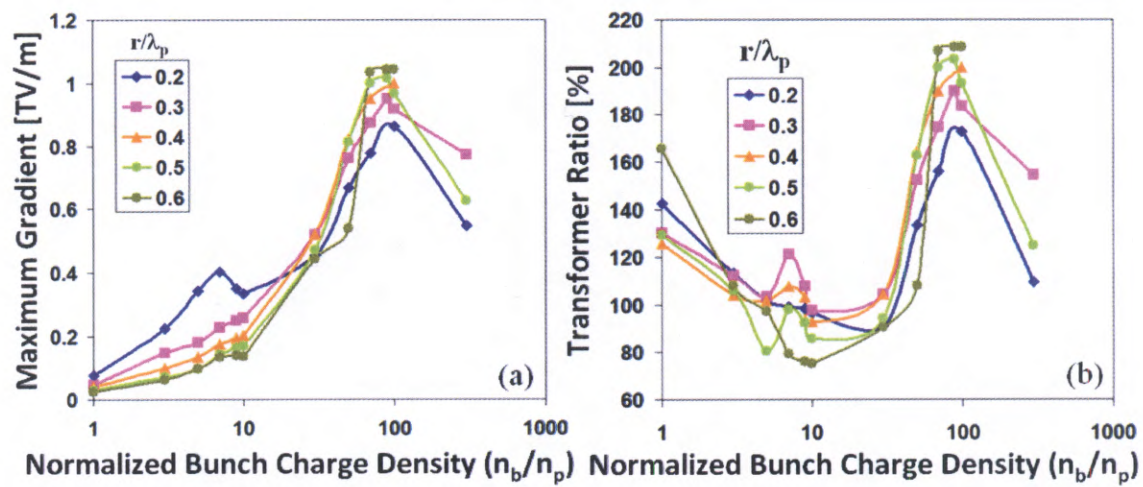


FIG. 7 (Y. M. SHIN)